Brain Structure and Function (2019) 224:1429–1446
https://doi.org/10.1007/s00429-019-01837-5

ORIGINAL ARTICLE

Neurochemically distinct circuitry regulates locus coeruleus activity during female social stress depending on coping style

Beverly A. S. Reyes[1] · Xiao-Yan Zhang[2] · Elsa C. Dufourt[1] · Seema Bhatnagar[2] · Rita J. Valentino[2] · Elisabeth J. Van Bockstaele[1]

Received: 27 June 2018 / Accepted: 16 January 2019 / Published online: 14 February 2019

Abstract

Stress-related psychiatric diseases are nearly twice as prevalent in women compared to men. We recently showed in male rats that the resident–intruder model of social stress differentially engages stress-related circuitry that regulates norepinephrine-containing neurons of the locus coeruleus (LC) depending on coping strategy as determined by the latency to assume a defeat posture. Here, we determined whether this social stress had similar effects in female rats. LC afferents were retrogradely labeled with Fluorogold (FG) and rats had one or five daily exposures to an aggressive resident. Sections through the nucleus paragigantocellularis (PGi), a source of enkephalin (ENK) afferents to the LC, and central nucleus of the amygdala (CeA), a source of corticotropin-releasing factor (CRF) afferents to the LC, were processed for immunocytochemical detection of c-fos, a marker of neuronal activity, FG and ENK or CRF. Like male rats, female rats defeated with a relatively short latency (SL) in response to a single resident–intruder exposure and showed significant c-fos activation of LC neurons, PGi-ENK LC afferents, and CeA-CRF-LC afferents. With repeated exposure, some rats exhibited a long latency to defeat (LL). LC neurons and CeA-CRF-LC afferents were activated in SL rats compared to control and LL, whereas PGi-ENK LC afferents were not. Conversely, in LL rats, PGi-ENK LC and CeA-CRF-LC afferents were activated compared to controls but not LC neurons. CRF type 1 receptor (CRF1) and μ-opioid receptor (MOR) expression levels in LC were decreased in LL rats. Finally, electron microscopy showed a relative increase in MOR on the plasma membrane of LL rats and a relative increase in CRF1 on the plasma membrane of SL rats. Together, these results suggest that as is the case for males, social stress engages divergent circuitry to regulate the LC in female rats depending on coping strategy, with a bias towards CRF influence in more subordinate rats and opioid influence in less subordinate rats.

Keywords Locus coeruleus · Social stress · Enkephalin · Corticotropin-releasing factor · Nucleus paragigantocellularis · Central nucleus of the amygdala · μ-Opioid receptor and corticotropin-releasing factor receptor

Introduction

Stress is a contributing factor to psychiatric vulnerability and neural substrates and systems that mediate stress responses have also been linked to affective disorders (Matsuzaki et al. 2011; Sutherland et al. 2010; Vicario et al. 2012; McEwen 1998; de Kloet et al. 2005). For example, activation of the norepinephrine (NE)-containing nucleus, locus coeruleus (LC) by the stress neuropeptide corticotropin-releasing factor (CRF) is a component of the stress response and its overactivity has also been implicated in stress-related psychiatric disorders (Wong et al. 2000; Gold and Chrousos 2002; Bissette et al. 2003). For humans, stress is often of a social nature and this can be modeled in rodents using the resident–intruder stress (Miczek et al. 1982; Teskey et al. 1984; Wood et al. 2009, 2015). The resident–intruder stress is an ethologically relevant model to examine mechanisms underlying stress-related psychiatric disorders (Avgustinovich et al. 2005, Wood et al. 2015). It produces long-lasting effects on behavioral, physiological, and neuroendocrine responses (Koolhaas et al. 1999; Nikulina et al.

✉ Beverly A. S. Reyes
bar62@drexel.edu

[1] Department of Pharmacology and Physiology, College of Medicine, Drexel University, 245 S. 15th Street, Philadelphia, PA 19102, USA

[2] Department of Anesthesiology and Critical Care Medicine, Children's Hospital of Philadelphia, Philadelphia, PA 19104, USA

1999, 2008). These include dysregulation of the hypothalamic–pituitary–adrenal axis, decreased social interaction, anxiety, anhedonia, and self-administration of drugs of abuse (Miczek et al. 2004; Rygula et al. 2005; Wood et al. 2010, 2012). An important feature of this model is the degree of individual variability in the magnitude of its consequences (Wood et al. 2009, 2010). The individual variability has been linked to different coping strategies (Wood et al. 2009, 2010; Reyes et al. 2015) based on the latency to assume the subordinate defeat posture (Wood et al. 2009, 2010). These prior studies were conducted in male rats. Rats that show defeat with a relatively short latency (SL) exhibit anhedonia, immobility in the forced swim test, decreased heart rate variability and dysregulated hypothalamic–pituitary–adrenal axis, features that are analogous to those reported in human depression, compared to the social stressed rats that exhibit a long latency (LL) and resist defeat (Wood et al. 2010, 2012, 2015). Notably, the latencies are bi-modally distributed and cluster into distinct populations, and whereas most rats exhibit the SL phenotype with an initial exposure, the LL phenotype develops with repeated exposure in a subpopulation (Wood et al. 2010).

In male rats, a single resident–intruder exposure activates LC neurons (Wood et al. 2010; Chaijale et al. 2013; Reyes et al. 2015). Considered as a major stress response system, LC-NE activation is critical in maintaining arousal and cognitive flexibility in response to acute stress (Berridge and Waterhouse 2003; Valentino and Van Bockstaele 2008). However, prolonged exposure of LC-NE system to stress has been associated in arousal-related symptoms of stress-related psychiatric disorders (Melia and Duman 1991; Grillon et al. 1996; Pietrzak et al. 2013). Notably, with repeated exposures, LC activation is more prominent in SL compared to LL rats (Reyes et al. 2015). Moreover, we determined that repeated resident–intruder stress engages neurochemically distinct afferents to the LC depending on the latency phenotype. The LC receives convergent synaptic input from CRF (Van Bockstaele et al. 1995, 1998; Tjoumakaris et al. 2003; Reyes et al. 2011; Kravets et al. 2015) and enkephalin (ENK) afferents (Drolet et al. 1992; Van Bockstaele et al. 1995). These two peptides are released during social and physiological stress to have opposing excitatory and inhibitory effects on LC activity, respectively (Curtis et al. 2001, 2012; Chaijale et al. 2013). With repeated social stress, inhibitory ENK afferents are favored in LL rats and excitatory CRF regulation is favored in SL rats (Reyes et al. 2015). Thus, in male rats, the establishment of different coping strategies is associated with changes in the circuitry that regulates the LC-NE system.

Given the high prevalence of stress-related psychiatric disorders in females compared to males, the present study was designed to determine whether social stress coping strategy was associated with a differential regulation of the LC of female rats that was similar to that seen in males. Rats were injected with fluorogold (FG) into the LC to identify afferents and exposed to either a single or five daily exposures to resident–intruder stress. CRF and ENK LC afferents that were activated by the stress as determined by c-fos were quantified. In addition, the effects of repeated social stress on CRF receptor type 1 (CRF1) and μ-opioid receptor (MOR) expression in the LC were determined by Western blot and the cellular localization of the receptors was determined by immunoelectron microscopy.

Materials and methods

Experimental animals

Female Sprague–Dawley rats initially weighing 275–300 g (Charles River, Wilmington, MA) were singly housed (20 °C, 12-h light, and 12-h dark cycle lights on 0700) and used in these experiments. Rats were randomly assigned to social defeat or control groups with ad libitum access to food and water. Animals were allowed to acclimate for at least 5 days prior to exposure to stress protocols. All studies were approved by the Children's Hospital of Philadelphia Institutional Animal Care and Use Committee and conformed to the guidelines set forth by the National Institutes of Health Guide for the Use of Laboratory Animals. All efforts were made to utilize only the minimum number of animals necessary to produce reliable scientific data, and experiments were designed to minimize any animal distress.

Social defeat (resident–intruder) paradigm and restraint

As previously published by our group (Wood et al. 2010; Chaijale et al. 2013; Ver Hoeve et al. 2013; Reyes et al. 2015), the repeated social defeat paradigm was adapted and modified from the resident–intruder model originally designed by Miczek (Miczek 1979). Specifically, we used lactating rats as resident animals considering that lactating females are likely to defeat other female rats (Flannelly and Flannelly 1987) and as we have previously shown (Ver Hoeve et al. 2013). A group of lactating Sprague–Dawley rats (Charles River Laboratories) were individually housed for use as resident animals in a resident–intruder paradigm to induce defeat. On each day, adult female experimental animals used as intruders were subjected to 30-min episodes of social defeat stress. Briefly, intruders were randomly placed in the home cage of unfamiliar lactating female Sprague–Dawley rat (650–850 g) that has been pre-screened for aggression and allowed to interact until the intruder displayed the supine defeat posture for approximately 3 s. Following a display of defeat posture

or at the end of 15 min if there was no display of defeat posture, the rats were separated by a wire mesh barrier for the remainder of the 30-min stress. The partition prevents further physical contact, but allows for exposure to auditory and olfactory stimuli. Control or unstressed rats were placed in a novel cage with a wire mesh barrier for 30 min during the time social defeat was occurring. At the end of 30 min, both experimental and control rats were returned to their home cages. There were minimal and infrequent injuries during the 15 min of physical interaction. Intruders were returned to their home cages and lactating mothers (residents) were reunited with their pups. For repeated social stress, the procedure was repeated everyday for 5 consecutive days with the intruder being exposed to different residents each day. The latency to assume defeat or the subordinate posture was recorded for each rat for each exposure to social defeat stress. The mean latency over the 5 days was calculated to each rat and analyzed by a cluster analysis across the group (JMP 0.0.0, SAS Institute; http://www.jmp.com).

Fluorogold injection into the locus coeruleus

Fluorogold injection into the LC was carried out as previously described for rats that served as intruders (Reyes et al. 2015). Intruder rats and matched controls were anesthetized with a 2% isoflurane—air mixture, positioned in a stereotaxic apparatus and prepared for electrophysiological localization of the LC using the glass micropipette. Micropipettes (glass 1BBL W/Fil, 1.2 mm in outer diameter; World Precisions Instruments, Inc., Sarasota, FL) with tip diameters of 15–20 µm were filled with a 2% solution of Fluorogold (FG; Fluorochrome) in 0.9% sterile saline. Microelectrode signals were led from a preamplifier to filters and additional amplifiers. Impulse activity was monitored on an oscilloscope and with a speaker to aid in localizing the LC. When neuronal activity characteristic of the LC was localized (spontaneous discharge rate of 1–4 Hz, entirely positive notched waveform of 2–3 ms duration in unfiltered trace and biphasic response to tail or paw pinch), the micropipette was repositioned until the core of the LC was located. Then, FG was iontophoresed (5 mA, 7 s duty cycle, 15 min) and the micropipette was kept in place for 10 min to prevent leakage. After iontophoresing FG into the LC core, the pipette was repositioned to the dorsolateral peri-LC dendritic field for an additional 15-min application of FG followed by a 10-min iontophoretic period. Finally, the micropipette was removed, and the scalp incision was sutured. After 3 days, rats were divided into groups and exposed to social stress or a control manipulation.

Specificity of receptor antisera

The characterization and specificity of the MOR antibody used in the present study were conducted in our previous reports (Surratt et al. 1994; Cheng et al. 1996; Van Bockstaele et al. 1996a, b). The rabbit polyclonal MOR was raised against a glutaraldehyde conjugate of the C-terminal 18 amino acids rat MOR and keyhole limpet hemocyanin that specifically recognizes immunocytochemical labeling for MOR within various brain regions using Western blotting, immunoprecipitation and light microscopic studies (Surratt et al. 1994; Van Bockstaele et al. 1996a, b). Immunolabeling was selectively absorbed with the appropriate peptide, with concentrations of 1 and 10 µg/ml (Van Bockstaele et al. 1996a). In addition, the specificity of MOR antibody was tested by probing rat heart lysates, which do not express MOR (Ventura et al. 1989; Peng et al. 2012). The CRF1 antibody was raised in rabbit.

The characterization and specificity of CRF1 antibody have been previously described using light and immunoelectron microscopic studies (Reyes et al. 2008). CRF1 immunolabeling was absent when using tissue sections from mice with CRF1 deletion, verifying that the CRF1 antibody detects CRF1 (Reyes et al. 2008). Using electron microscopy demonstrating the CRF-induced internalization of the CRF1 protein recognized by this antiserum is consistent with the concept that the protein is a CRF receptor, as it is less likely that exposure to CRF would elicit internalization of another plasma membrane bound protein (Reyes et al. 2006, 2008). In addition, we previously showed that the selective CRF_1 antagonist interferes with internalization of the protein recognized by the antiserum supporting the evidence of specificity of the CRF1 antibody (Reyes et al. 2006).

The mouse monoclonal antibody raised against opioid peptide leucine^5-enkephalin (Leu-ENK) was shown to react primarily with Leu-ENK, but also cross-react slightly with methionine^5-ENK. The Leu-ENK antibody has been characterized using preadsorption controls (Barr and Van Bockstaele 2005; Milner et al. 1995). In addition, tissue sections that were processed in parallel without the primary antibody did not exhibit ENK immunoreactivity (Barr and Van Bockstaele 2005; Reyes et al. 2005).

The c-fos antibody is a mouse monoclonal antibody raised against amino acids at the C-terminus of c-fos of human origin. With a molecular weight of 62 kDa, the specificity of c-fos antibody was characterized by preabsorbing the primary antiserum with a peptide corresponding to the DNA-binding region of c-fos protein (amino acids 127–154), which is highly conserved between c-fos and fos-related proteins (Ghosal et al. 2010; Jia et al. 2011; Por et al. 2010). The rabbit c-fos antibody is generated against synthetic peptide sequence corresponding to amino acid 4–17 of human c-fos and recognizes the N-terminus of c-fos, with the molecular

weight of − 55 kDa. The specificity of c-fos antibody has been tested by absorbing it with the c-fos peptide (Dai et al. 2005; Noga et al. 2011). Furthermore, when rabbit c-fos or mouse c-fos antibody was omitted at a dilution of c-fos primary antisera, no immunoreactivity was observed (Retson et al. 2015; Reyes et al. 2015).

Immunohistochemistry

Rats were deeply anesthetized with 5% isoflurane and transcardially perfused through the ascending aorta with 2% heparinized saline, followed with 4% formaldehyde in 0.1 M phosphate buffer (PB; pH 7.4), 90 min after the last experimental manipulation. Brains were then removed and post-fixed in 4% formaldehyde overnight at 4 °C and stored in sucrose solutions of 10% and 20% for 1 h each, followed by 30% sucrose for 48,072 h in (PB) containing sodium azide at 4 °C. One side of the brain was notched to verify tissue orientation following sectioning. Forty-micrometer-thick frozen sections through the LC were cut in the coronal plane in a sequential manner using a freezing microtome and collected in 0.1 M PB. Every fourth section through the rostro-caudal extent of the LC was collected and processed for immunoperoxidase detection of the extent of the FG injection site. Similarly, serial coronal sections through the PGi and CeA were processed for immunoperoxidase visualization of FG to evaluate the magnitude of retrograde labeling. These sections were rinsed extensively in 0.1 M tris-buffered saline (TBS; pH 7.6). Sections were then incubated in 0.5% bovine serum albumin (BSA) and 0.25% Triton X-100 in 0.1M TBS for 30 min and rinsed extensively in 0.1 M TBS.

Sections were incubated in rabbit anti-FG (1:2000; Chemicon International Inc., Temecula, CA) for 15–18 h at room temperature. They were then rinsed three times in 0.1 M TBS and incubated in biotinylated donkey anti-rabbit (1:400; Jackson ImmunoResearch Laboratories, Inc., West Grove, PA, USA) for 30 min followed by rinses in 0.1 M TBS. Subsequently, sections were incubated for 30 min in avidin–biotin complex (Vector Laboratories, Burlingame, CA, USA). FG was visualized by a 9-min reaction in 22 mg of 3,3′-diaminobenzidine and 10 µl of 30% hydrogen peroxide in 100 ml of 0.1 M TBS. Sections were collected, dehydrated, and coverslipped for light microscopic analysis of FG immunoreactivity.

A series of sections through the rostro-caudal segment of the PGi was processed for immunocytochemical visualization of FG, c-fos, and ENK and a series of sections through the CeA was processed for immunocytochemical visualization of FG, c-fos, and CRF. Eleven animals with the most restricted placement of FG and optimal retrograde labeling were used in the analysis. Free-floating sections were rinsed extensively in 0.1 M PB followed by rinses in 0.1 M TBS. Sections were then incubated in 0.5% BSA in 0.1 M TBS for 30 min, and rinsed in 0.1 M TBS for 10 min, three times. Following rinses, sections containing the PGi were incubated overnight at room temperature in a solution containing guinea pig anti-FG (1:2000; Protos Biotech Corp., New York, NY), rabbit anti-c-fos (1:3000; Calbiochem), and mouse anti-Leu-ENK (1:100; Fitzgerald Laboratories, Concord, MA) in 0.1M TBS with 0.1% BSA and 0.25% Triton X-100. Likewise, tissue sections from the CeA were incubated overnight at room temperature in rabbit anti-FG (1:2000; Chemicon International Inc.), mouse anti-c-fos (1:100; Santa Cruz Biotechnology Inc., Santa Cruz, CA) and guinea pig anti-CRF (1:2000; Peninsula Laboratories, San Carlos, CA). Sections were then washed in 0.1 M TBS and sections containing the PGi were incubated in a secondary antibody cocktail containing fluorescein isothiocyanate (FITC) donkey anti-rabbit (1:200; Jackson ImmunoResearch Laboratories Inc., West Grove, PA, USA), tetramethyl rhodamine isothiocyanate (TRITC) donkey anti-mouse (1:200; Jackson ImmunoResearch) and AlexaFluor 647 donkey anti-guinea pig (1:200; Jackson ImmunoResearch) antibodies prepared in 0.1% BSA and 0.25% Triton X-100 in 0.1 M TBS for 2 h in the dark. Sections from the CeA were incubated in a secondary antibody cocktail containing FITC donkey anti-mouse (1:200; Jackson ImmunoResearch Laboratories Inc.), TRITC donkey anti-guinea pig (1:200; Jackson ImmunoResearch) and AlexaFluor 647 donkey anti-rabbit (1:200; Jackson ImmunoResearch) antibodies. Following incubation with the secondary antibodies, the tissue sections were washed thoroughly in 0.1 M TBS, mounted on slides and allowed to dry in complete darkness. The slides were dehydrated in a series of alcohols, soaked in xylene and coverslipped using DPX (Sigma-Aldrich Inc.). Sections were visualized using an Olympus 1×81 laser microscope (Olympus, Hatagaya, Shibuya-Ku, Tokyo, Japan) and images captured using Olympus Fluoview ASW FV1000 program (Olympus, Hatagaya, Shibuya-Ku, Tokyo, Japan).

As an indication of stress-induced LC activation, c-fos immunoreactivity was also quantified in every fourth section through the LC. Free-floating sections were rinsed in 0.1 M PB followed by rinses in 0.1 M TBS. Subsequently, tissue sections were incubated in 0.5% BSA in 0.1 M TBS for 30 min and rinsed in 0.1 M TBS for 10 min, three times. Tissue sections were then incubated overnight in a rabbit monoclonal antibody for c-fos (1:3000; Calbiochem) in 0.1% BSA and 0.25% Triton X-100 in 0.1 M TBS. Incubation time was 15–18 h in a rotary shaker at room temperature. Following 15–18 h of incubation, tissue sections were rinsed three times in 0.1 M TBS and incubated in biotinylated donkey anti-rabbit (1:400 Jackson ImmunoResearch Laboratories) for 30 min followed by rinses in 0.1 M TBS. Following rinses, tissue sections were incubated for 30 min in avidin–biotin complex (ABC Elite Kit, Vector Laboratories, Burlingame, CA) solution at room temperature. The

tissue sections were then immersed for 4 min in a solution containing 22 mg of 3–3′ diaminobenzidine (DAB; Aldrich, Milwaukee, WI) and 10 µl of 30% hydrogen peroxide (H_2O_2) in 100 ml of 0.1 M TBS. A total of six sections were analyzed per rat and the mean number per group was obtained by determining the average c-fos-immunoreactive cells per section per rat. The mean number per rat was determined for comparison between groups. For the acute social stress (1 day defeat), the number of c-fos immunoreactive neurons (c-fos single labeling) was analyzed using the Student's *t* test. For the repeated social stress (5-day defeat), the number of c-fos immunoreactive neurons (c-fos single labeling) was analyzed using a one-way analysis of variance (ANOVA) followed by a posthoc analysis.

Controls and data analysis

Sections from each rat were first examined for accurate and localized FG injections determined from the bright-field images (Olympus BX51). Images were captured using Spot Advanced software (Diagnostic Instruments). The discrete LC injection placements in this study filled the LC core and dorsolateral peri-LC, where LC dendritic processes are distributed. FG LC injections yielded retrograde labeling in the PGi and CeA reflecting afferent input to the LC consistent with the previous tract tracing studies (Drolet et al. 1992; Van Bockstaele et al. 1996c, 1998; Reyes et al. 2011, 2015). Rats that received optimal FG LC injections and exhibited retrograde labeling in the PGi and CeA were used in the analysis. Regardless of whether social defeat was acute or chronic, the characteristics of LC injections and retrograde labeling in the PGi and CeA were similar. In other words, the FG injection targeted the LC including the core and to some extent the peri-LC (Fig. 1aii) and similar retrograde labeling was evident in the neurons in the PGi (Fig. 1bii) and CeA (Fig. 1cii). The area of the PGi that was analyzed extends from the anterior pole of the lateral reticular nucleus to the level of the caudal third of the facial nucleus, as previously described (Andrezik et al. 1981, Plates 62–68; Paxinos and Watson 1998). The area of the CeA analyzed is located in the medial part of the amygdaloid complex which is bounded laterally by the basolateral amygdaloid nucleus, lateral amygdaloid nucleus, and amygdaloid intermedullary gray, medially by primary substantia innominata and medial amygdaloid nucleus, dorsally by the basal nucleus and interstitial nucleus of the posterior limb of the anterior commissure, and ventrally by the intercalated amygdaloid nucleus and intra-amygdaloid division of the bed nucleus of stria terminalis (Plates 25 through 30; Paxinos and Watson 1998). For quantification, every fourth coronal (120 µm apart) section was taken through the anteroposterior extent of the PGi and CeA. The number of c-fos, FG, ENK, or CRF, dually labeled cells (FG/c-fos) and triple-labeled cells (FG, c-fos, and ENK or CRF) was counted in 12 PGi-containing sections and six CeA-containing sections. The total number of labeled (FG, c-fos, Enk or CRF, FG/c-fos, and FG/c-fos/ENK, or FG/c-fos/CRF) was obtained and the data were analyzed using a one-way ANOVA with Tukey posthoc tests for comparison between individual groups (JMP 9.0.0, SAS Institute). In addition, using GraphPad Prism 6, correlation studies were conducted in the number of c-fos in LC, triple-labeled neurons in the PGi/CeA, CRF1 protein expression in LC, MOR protein expression in LC, MOR cytoplasmic:total ratio in LC and CRF1 cytoplasmic:total ratio in LC, in correlation with the defeat latency.

Western blot

Female rats randomly assigned to either social defeat ($n = 11$) or control manipulation ($n = 5$) were decapitated and extracted brains were snap-frozen in dry ice and placed at − 80 °C until used. The CRF1 and MOR protein levels in LC tissue were quantified by Western blotting as previously described (Bangasser et al. 2010; Guajardo et al. 2017). The frozen brain was cut on a cryostat and whole LC tissue punches were taken (1 mm) bilaterally using a trephine. These were stored at − 80 °C until use. Tissue samples were homogenized, sonicated, and centrifuged and supernatant was collected as previously described (Bangasser et al. 2010; Guajardo et al. 2017). Protein content was determined using the BCA method. Protein extracts (15 µg) were subjected to SDS-PAGE gel electrophoresis and transferred to polyvinylidene fluoride membranes (Immobilon-FL). Membranes were blocked with Odyssey Buffer (diluted in PBS 1:1) and incubated with the following primary antibodies: goat anti-CRF1/2 (1:500; Santa Cruz Biotech, Santa Cruz, CA), rabbit anti-MOR (1:1000; Chemicon, Temecula, CA), and rabbit anti GAPDH (1:5000) or mouse anti-β-actin (1:5000). After rinses, membranes were incubated with the following fluorescent secondary antibodies: donkey anti-goat for CRF1/2 (1:5000, IRDye 800CW, LiCor), donkey anti-rabbit for detection of MOR (1:5000, IRDye 800CW, LiCor), donkey anti-rabbit for GAPDH (1:5000), and donkey anti-mouse for β-actin (1:5000). Membranes were scanned and Odyssey Infrared Imaging software quantified the integrated intensity of each band and determined molecular weights based on Biorad Precision Plus Protein Standards. The ratios of CRF1:GAPDH and MOR:β-actin were calculated and the mean ratios were statistically compared between groups using a one-way ANOVA with Tukey posthoc tests for comparison between individual groups (JMP 9.0.0, SAS Institute). Duplicate or triplicate samples were averaged for an individual rat.

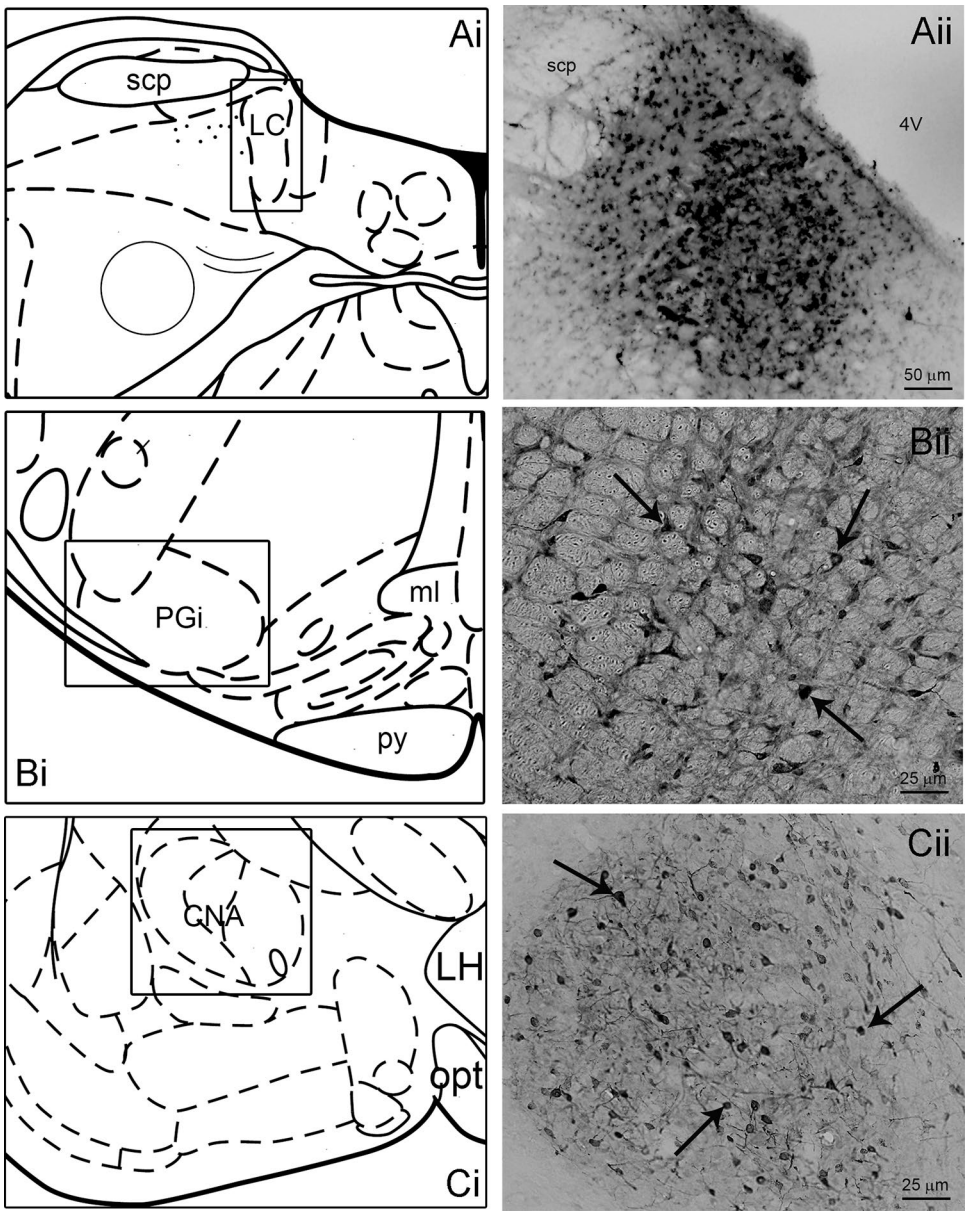

Fig. 1 Fluorogold injection into the locus coeruleus and retrograde labeling in the nucleus paragigantocellularis (PGi) and central nucleus of the amygdala (CeA). **ai–ci**. Schematic diagram adapted from the rat brain atlas (Paxinos and Watson 1998) depicting the anteroposterior levels of the representative injection site (**a**). Following FG injection into the LC, a representative bright-field photomicrograph showing the FG retrograde labeling in the nucleus PGi (Bii at bregma − 12.30 mm and bregma − 13.68; Paxinos and Watson 1998) and CeA (Cii at bregma − 2.12; Paxinos and Watson 1998). The arrows indicate immunoperoxidase labeled cells. Scale bars: **a** 50 µm; **b, c** 25 µm

Immunoelectron microscopy

Following to exposure to social defeat paradigm, rats were deeply anesthetized with sodium pentobarbital (60 mg/kg) and perfused transcardially through the ascending aorta with 10 ml heparinized vehicle followed with 50 ml of 3.75% acrolein (Electron Microscopy Sciences, Fort Washington, PA, USA) and 200 ml of 2% formaldehyde in 0.1 M PB. The brains were cut into 1–3 mm coronal slices, post-fixed and sections (40 µm) were cut through the LC using a Vibratome (Technical Product International, St. Louis, MO, USA). The tissue sections were incubated in rabbit anti-MOR (1:2500; Chemicon, Temecula, CA) or rabbit anti-CRF1 (1:200; Santa Cruz Biotechnology Inc., Santa Cruz, CA) in 0.1 TBS with 0.1% BSA for 18–20 h at room temperature. Sections were incubated in goat anti-rabbit IgG ultra-small conjugate (1:100; Amersham Bioscience Corp., Piscataway, NJ, USA) at room temperature for 2 h. A silver enhancement kit (Amersham Bioscience Corp.) was used for silver intensification of the gold particles. Sections were flat embedded in Epon 812 (Electron Microscopy Sciences); (Leranth and Pickel 1989) and thin sections (50–80 nm) were cut from the outer surface of the tissue, collected on grids. Sections were collected on copper mesh grids, examined with an electron microscope (Morgagni, Fei Company, Hillsboro, OR, USA) and digital images were captured using the AMT advantage HR/HR-B CCD camera system (Advance Microscopy Techniques Corp., Danvers, MA, USA). For quantification, tissue sections were taken from three to five rats per group with the

good preservation of ultrastructural morphology. The ratio of cytoplasmic to total immunogold–silver particles for each dendrite (110 dendrites for each rat per group) and the mean ratio was determined per rat. The average of the ratio for each rat in experimental group was obtained as the group mean and these were compared between groups by ANOVA followed by Tukey posthoc tests for comparison between individual groups (JMP 9.0.0, SAS Institute). Figures were assembled and adjusted for brightness and contrast in Adobe Photoshop.

Results

Defeat latencies

Consistent with our previous reports (Reyes et al. 2015; Wood et al. 2010), repeatedly stressed rats clustered into two populations based on either a relatively SL or LL to assume the subordinate defeat posture. The range of latencies for the SL rats was 69–110 s with a mean latency of 87 ± 7 s ($n = 6$). The range of latencies for LL rats was 524–644 s with a mean latency of 571 ± 37 s ($n = 3$) and this was significantly different from the mean latency of SL rats ($p \leq 0.0001$).

Retrograde labeling

Fluorogold injections in the LC effectively defined retrogradely labeled cells in the PGi and CeA. Fourteen rats with targeted placement of FG in the LC and prominent retrograde transport were selected for analysis. Figure 1aii shows a representative bright-field photomicrograph depicting an FG injection site into the LC. FG injection sites were visualized by a dark area of peroxidase reaction product within the boundaries of the LC. Injections targeted the region of the LC at the level bounded medially by the wall of the fourth ventricle, laterally by the mesencephalic trigeminal tract, ventrally by the Barrington's nucleus and dorsally by the superior cerebellar peduncle (Fig. 1ai). The characteristics of the FG deposits in the LC and retrograde labeling of the neurons of the PGi (Fig. 1bii) and CeA (Fig. 1cii) were evident and similar to those that we previously reported (Drolet et al. 1992; Van Bockstaele et al. 1995, 1998; Reyes et al. 2005, 2015; Kravets et al. 2015). To determine that FG targeted LC neurons, some sections with optimum FG injection in the LC were processed for dual immunohistochemistry. Dual immunolabeling of FG and TH in the LC showed that FG targeted TH-containing neurons in the LC, where FG was labeled with FITC (green), while TH was labeled with TRITC (red; Fig. 2).

Acute social stress-induced activation of LC neurons and ENK and CRF afferents

All female rats exposed to a single episode with the resident intruder had relatively short latencies to defeat [58.5 ± 14; s ($n = 6$)] similar to the previous report in males (Wood et al. 2010, 2012, 2015). A single resident–intruder exposure robustly increased the number of LC neurons that were c-fos immunoreactive (Fig. 3). The mean number of c-fos immunoreactive neurons in the LC of stressed rats was 245 ± 12 ($n = 6$) compared to 46 ± 8 ($n = 5$) control rats ($p < 0.01$). Some sections were labeled with c-fos and TH to determine if LC neurons were expressing c-fos immunoreactivity. Figure 4 shows that c-fos labeled with FITC (green) was expressed in TH-labeled neurons (red; labeled with TRITC) in LC.

Single exposure to the resident intruder did not affect total numbers of FG-retrogradely labeled neurons in the PGi ($p = 0.052$; Table 1) or CeA ($p = 0.051$; Table 1), confirming our previous report in males (Reyes et al. 2015). However, a single exposure to social stress increased number of c-fos immunoreactive cells compared with control manipulation in both the PGi ($p < 0.01$; Table 1) and the CeA ($p < 0.01$; Table 1). Similarly, single exposure to social stress increased the number of ENK-immunoreactive neurons that contained FG and c-fos in the PGi ($p < 0.01$; Fig. 5; Table 1) and CRF-immunoreactive neurons that contained FG and c-fos in the CeA ($p < 0.01$; Fig. 5; Table 1) compared to controls. Rats exposed to single exposure to social stress demonstrated evidence of both greater ENK and CRF drive to the LC from the PG1 ($p < 0.01$; Fig. 5; Table 1) and CeA ($p < 0.01$; Fig. 5; Table 1), respectively, compared with controls. The percentage of LC-projecting neurons from the PGi and CeA that contained ENK ($p < 0.01$) or CRF ($p < 0.01$) immunoreactivity, respectively, was also greater in stressed compared with control rats.

Repeated social stress-induced activation of LC neurons and ENK and CRF afferents

The mean number of retrogradely labeled neurons following repeated social stress was similar between experimental groups in the PGi [$F_{(2,13)} = 0.99$; $p = 0.4$] and CeA [$F_{(2,13)} = 0.1$; $p = 0.91$; Table 1]. Repeated resident–intruder increased the number of c-fos immunoreactive LC neurons in SL rats only (Fig. 6). The mean number of c-fos immunoreactive neurons for SL rats was 65 ± 5 compared to 33 ± 6 for control and 35 ± 6 for LL rats. Statistical analysis showed that there was a significant negative correlation ($R = 0.7085$; $F = 17.01$; $p = 0.0044$) between the c-fos expressing neurons in LC compared to defeat latency (Fig. 7a), indicating that as the latency of defeat progresses, the number of c-fos immunoreactive neurons decreases. Figure 5a shows examples of

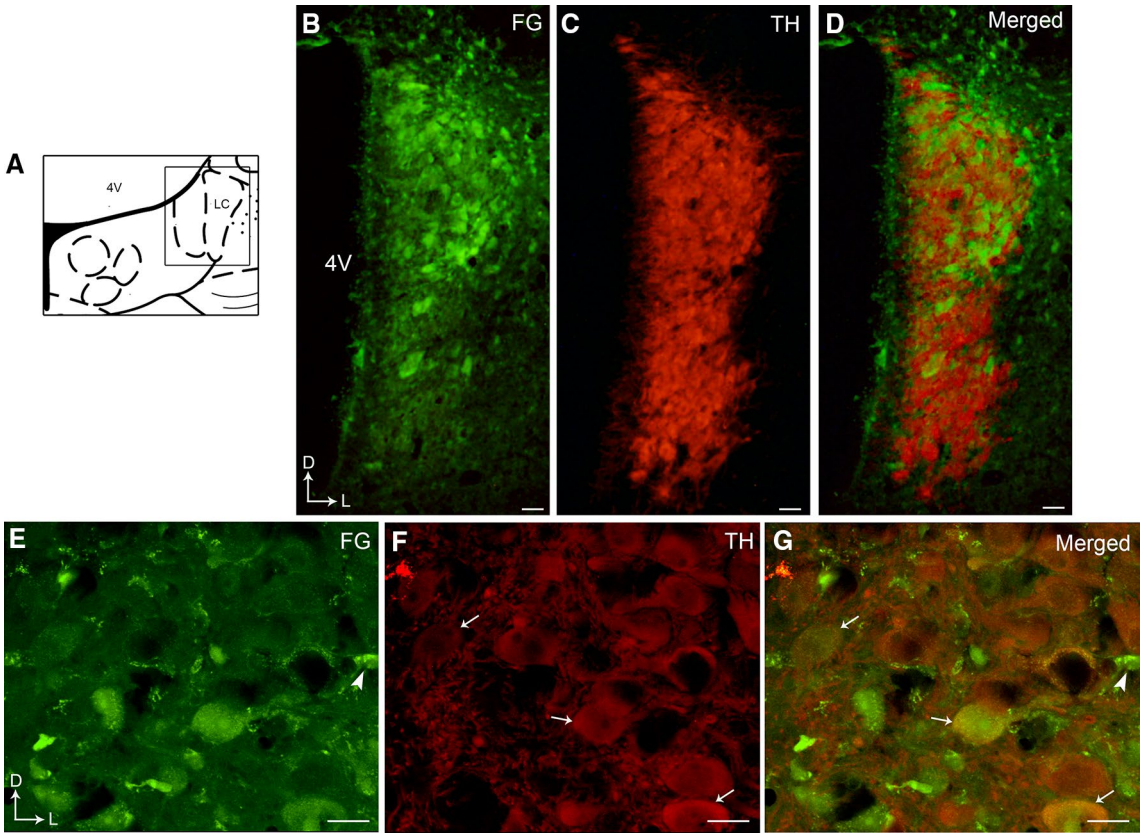

Fig. 2 Low (**b**–**d**) and high (**e**–**g**) magnification confocal immunofluorescence photomicrographs showing FG and TH immunoreactivities in the LC. **b, e** FG immunolabeling was detected by fluorescein isothiocyanate (green). **c, f** TH was detected by rhodamine isothiocyanate (red). **d, g** Merged image. Arrows point to FG and TH-containing neurons. Arrowhead point to singly labeled FG-containing neuron. Corner arrows indicate dorsal (D) and lateral (L) orientation. *4V* fourth ventricle. Scale bar, **b**–**d** 50 µm; **e**–**g** 25 µm

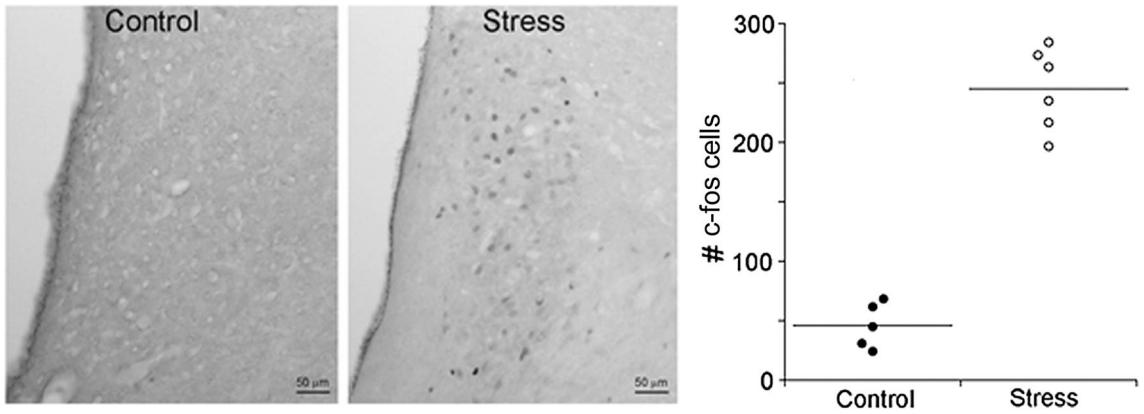

Fig. 3 Activation of locus coeruleus (LC) neurons following single exposure to resident–intruder stress. Representative sections from rats exposed to a single control manipulation (control) and a single resident–resident intruder stress (stress). Scatterplot showing the number of c-fos profiles in the LC after a single stress ($n=6$) or control manipulation ($n=5$) for individual control and stressed rats. Lines through the points indicate the group mean

triple-labeled neurons expressing FG, ENK, and c-fos in the PGi. A distinction in PGi neuronal activation was evident between rats with different coping strategies following repeated exposure to social stress. As evidenced by the total number of c-fos immunoreactive neurons, more PGi neurons were activated in LL rats compared with control and

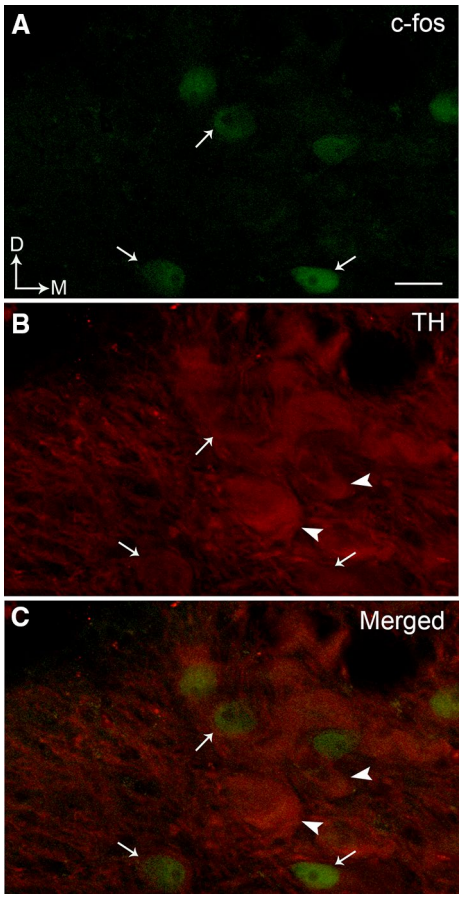

Fig. 4 High magnification confocal immunofluorescence photomicrographs showing c-fos and TH immunoreactivities in the LC (**a**–**c**). **a** c-fos immunolabeling was detected by fluorescein isothiocyanate (green). **b** TH was detected by rhodamine isothiocyanate (red). **c** Merged image. Arrows point to c-fos within TH-containing neurons. Arrowheads point to singly labeled TH neurons. Corner arrows indicate dorsal (D) and lateral (L) orientation. Scale bar, 25 µm

SL rats [$F_{(2,13)}=5$; $p\leq0.05$; Table 1]. In addition, the number of PGi-ENK neurons that project to the LC was greater in LL rats compared with control and SL [$F_{(2,13)}=54.6$; $p\leq0.00001$; Table 1]. Importantly, a greater number of PGi neurons that project to the LC were activated in LL rats compared to control and SL rats [$F_{(2,13)}=16.9$; $p\leq0.0005$; Table 1]. Indeed, there was a greater ENK-drive to the LC in LL rats compared with SL and control rats as indicated by a greater percentage of retrogradely labeled c-fos expressing neurons that also expressed ENK immunoreactivity [$F_{(2,13)}=8.4$; $p\leq0.006$; Table 1]. Triple-labeled neurons expressing c-fos, FG and ENK in the PGi were then compared to the latency of defeat using correlation analysis, as shown in Fig. 7b. Statistical analysis showed that there was a significant positive correlation ($r=0.8846$; $p=0.0022$). This result demonstrates a relationship between c-fos, FG, and ENK and defeat latency indicating that as latency of defeat prolongs, the number of triple-labeled neurons in the PGi increases.

Figure 5b shows examples of triple-labeled neurons expressing FG, CRF, and c-fos in the CeA following chronic social defeat exposure. In direct contrast to the patterns of activation within the PGi, more CeA neurons were activated in SL rats compared with control or LL rats based on the number of neurons exhibiting c-fos immunoreactivity [$F_{(2,13)}=8.9$; $p\leq0.005$; Table 1]. Interestingly, CeA-CRF neurons that project to the LC were more numerous in the CeA of SL rats compared with control or LL rats [$F_{(2,13)}=7.2$; $p\leq0.01$; Table 1]. Importantly, a greater number of CeA-CRF neurons that project to the LC are activated in SL compared to control or LL rats [$F_{(2,13)}=20.4$; $p\leq0.0002$; Table 1]. In addition, SL rats showed greater activation of CRF-LC-projecting neurons compared to other groups as also indicated by the percentage of CRF-immunolabeled LC-projecting neurons exhibiting c-fos immunolabeling compared with both controls and LL rats [$F_{(2,13)}=7.2$; $p\leq0.01$; Table 1]. There was no significant correlation between the triple-labeled neurons expressing c-fos, FG and CRF in the CeA and defeat latency [($r=0.2468$; $p=0.1737$); Fig. 7c].

Repeated social stress alters MOR and CRF1 protein expression levels and trafficking in the LC

Defeat latencies in rats used for Western blot studies ranged between 41 and 143 s with a mean latency of 93 ± 19 s ($n=6$). The range of latencies for LL rats was 308–1008 s with a mean latency of 236 ± 96 s ($n=6$) and this was significantly different from the mean latency of SL rats, 129 ± 39 and ranged between 41 and 268 s ($p\leq0.001$). Quantification of MOR protein levels using Western blot analysis showed that repeated social stress decreased MOR levels in the LC of LL rats compared to SL rats ($p<0.002$) and control rats [$F_{(2,16)}=11.8$; $p<0.001$; Fig. 8]. There was a negative correlation between the MOR expression levels and latency to defeat, such that as the defeat latency progresses, the MOR expression levels decrease (Fig. 9a, $r=0.5489$; $p=0.0091$). CRF1 protein levels were decreased in the LC of LL rats exposed to social defeat compared to SL rats [$F_{(2,16)}=2.83$; $p<0.02$; Fig. 8] and tended to decrease compared to control rats [$F_{(2,16)}=2.83$; $p<0.09$; Fig. 8]. Similarly, there was negative correlation between CRF1 protein levels and latency to defeat, showing that as the defeat latency is prolonged the CRF1 protein level decrease [Fig. 9b, $r=0.5092$; $p=0.0137$].

Representative electron photomicrographs showing immunogold–silver labeling for MOR and CRF1 are presented in Fig. 10. Semi-quantitative analysis revealed that there was a lower ratio of cytoplasmic:total immunogold MOR labeling [$F_{(2,12)}=21.30$; $p<0.0001$; Fig. 11] in LL

Table 1 Number of labeled cells

	PGI					
	FG	c-fos	ENK	FG-c-fos	FG-ENK	FG-c
fos-ENK						
Control	126 ± 5	41 ± 6	220 ± 10	18 ± 3	NC	6 ± 1
Stress	139 ± 6	65 ± 6*	239 ± 7	23 ± 3	NC	16 ± 2***
Control	100 ± 12	19 ± 4	202 ± 9	11 ± 3	70 ± 11	1 ± 1
SL	97 ± 8	28 ± 4	212 ± 9	4 ± 2	87 ± 7	1 ± 0
LL	117 ± 12	52 ± 13*	209 ± 17	29 ± 4*#	102 ± 9	10 ± 1***,###
	CeA					
	FG	c-fos	CRF	FG- c-fos	FG-CRF	FG- c
fos-CRF						
Control	224 ± 7	86 ± 7	135 ± 5	31 ± 5	NC	8 ± 1
Stress	216 ± 9	182 ± 9***	220 ± 8***	53 ± 6*	NC	41 ± 5***
Control	187 ± 22	82 ± 17	200 ± 23	32 ± 6	51 ± 10	7 ± 3
SL	177 ± 28	161 ± 13*	258 ± 21	68 ± 12	92 ± 6	50 ± 11*,#
LL	197 ± 42	101 ± 11	239 ± 31	43 ± 10	75 ± 11	18 ± 3

For top table (PGi): ***$p < 0.001$, *$p < 0.05$, #vs Control and SL, ###vs Control and SL; one-way ANOVA comparisons

For bottom table (CeA): ***$p < 0.001$, *$p < 0.05$, #vs Control and LL; one-way ANOVA comparisons

rats compared to control and SL rats, indicating that MOR remained localized along the plasmalemma in LL rats. Moreover, semi-quantitative analysis of CRF1 revealed that there was a lower ratio of cytoplasmic:total immunogold CRF1 labeling [$F_{(2,12)} = 8.925$; $p < 0.0042$; Fig. 11] in SL rats compared to control and LL rats indicative of predominant localization of CRF1 along the plasma membrane in SL. While the ratio of cytoplasmic:total immunogold MOR labeling was negatively correlated with defeat latency [Fig. 9; $r = 0.7305$; $p = 0.0033$], the ratio of cytoplasmic:total immunogold CRF1 labeling was positively correlated with defeat latency [Fig. 9; $r = 0.5833$; $p = 0.0166$].

Discussion

The present studies provide neuroanatomical evidence demonstrating that in female rats, both CeA-CRF and PGi-ENK afferents to the LC are engaged during acute resident–intruder stress and there is a net activation of LC neurons. However, with repeated resident–intruder stress, distinct coping strategies emerge that are associated with strategy-specific changes in the circuitry, such that in the subpopulation of rats resisting subordination (LL), the stressor no longer activates LC neurons. This can be explained by the loss of activation of excitatory CeA-CRF afferents to the LC in the face of significant activation of inhibitory PGi-ENK afferents to the LC. In contrast, for subordinate-prone SL rats, excitatory CeA-CRF afferents but not PGi-ENK afferents are engaged by repeated stress, resulting in a net LC neuronal activation. These findings in females corroborate the neuroanatomical evidence that we previously reported in male rats following acute and chronic resident–intruder stress exposure (Reyes et al. 2015). That similar results were obtained in both sexes underscores that repeated social stress favors opioid inhibitory regulation of the LC in rats that resist subordination and CRF excitatory regulation of the LC in subordinate–prone rats. Opposing regulation of LC activity based on coping strategy may underlie differential stress vulnerability in different coping phenotypes. A potential sex difference in the response to repeated stress lies in the regulation of MOR protein levels in the LC and receptor trafficking, although these need to be further examined in studies that directly compare males and females.

Methodological considerations

Certain factors inherent to retrograde tract tracing and immunolabeling of neuropeptides need to be considered in interpretating the present results. An important consideration is related to the extent and localization of the FG injection, which cannot be uniform across rats because of individual variations in the injection and uptake of FG. This variability is minimized in the present study by accurate electrophysiological localization of the FG pipette (Curtis et al. 1997). To minimize diffusion and limit the degree of damage and uptake by fibers of passage, FG was delivered using iontophoresis through small diameter micropipettes rather than pressure injection (Curtis et al. 1997; Reyes et al.

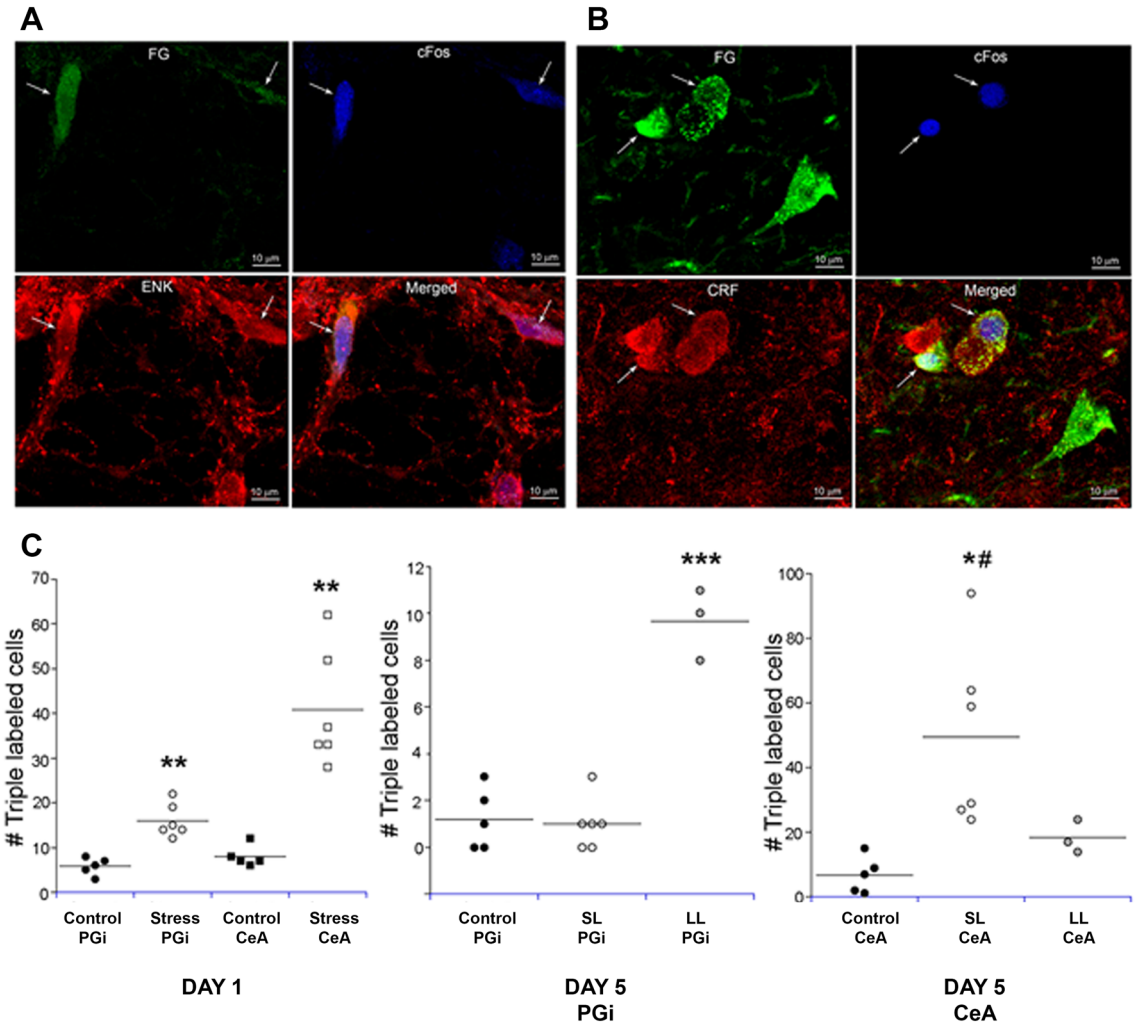

Fig. 5 Activation of locus coeruleus (LC)-projecting enkephalin neurons in the nucleus PGi (**a**) and LC-projecting CRF neurons in the CeA (**b**). **a** Representative high magnification immunofluorescence photomicrographs from a long latency (LL) rat showing LC-projecting neurons in the PGi. c-fos is labeled in blue, FG immunolabeling is labeled in green and ENK-immunolabeling is labeled in red. The merged image shows all labels. Arrows point to the same triple-labeled neuron in all images. Scale bar, 10 µm. **b** Representative high magnification immunofluorescence photomicrographs from a SL rat showing LC-projecting neurons in the CRF. c-fos is labeled in blue, FG immunolabeling is labeled in green and CRF-immunolabeling is labeled in red. The merged image shows all labels. **c** Scatterplot showing triple-labeled cells on day 1 (single stress: $n=6$; control: $n=5$) and day 5 (control: $n=5$; SL: $n=6$; LL: $n=3$) in the PGi and CeA, respectively. Lines through the points indicate the group mean. Arrows point to the same triple-labeled neuron in all images. Scale bar, 10 µm. Scatter plot on the left showing the number of triple-labeled cells that were also immunolabeled with ENK and CRF, respectively, for individual control and defeat group following 1 day of social stress exposure. Middle scatter plot showing the number of triple-labeled cells that were also immunolabeled with ENK for individual control, long latency (SL) and long latency (LL) following repeated social stress exposure. Scatter plot on the right showing the number of triple-labeled cells that were also immunolabeled with CRF for individual control, SL and LL following repeated social stress exposure

2006). It should be noted that the quantification of the CRF and ENK neurons may be underestimated, because rats did not receive colchicine, which optimizes peptide visualization, but affects c-fos expression and interferes with retrograde labeling (Gorenstein et al. 1985; Monti-Graziadei and Berkley 1991; Rite et al. 2003). Despite this, ENK and CRF-labeled neurons were clearly visualized in cases analyzed.

We have recently reported that the number of MOR immunogold silver particles in naïve female rats regardless of the phase of estrous cycle is comparable (Enman et al. 2018). In addition, our previous reports of receptor trafficking in the LC showed that the circulating gonadal hormones are not associated in sex differences in CRF1 function (Bangasser et al. 2010; Retson et al. 2015). In addition, it has been established that stress dysregulates estrous cyclicity (Ehnert and Moberg 1991; Gonzalez et al. 1994; Li et al. 2014; Marchlewska-Koj et al. 1994), since stress suppresses luteinizing hormone secretion (Breen et al. 2008; Pierce

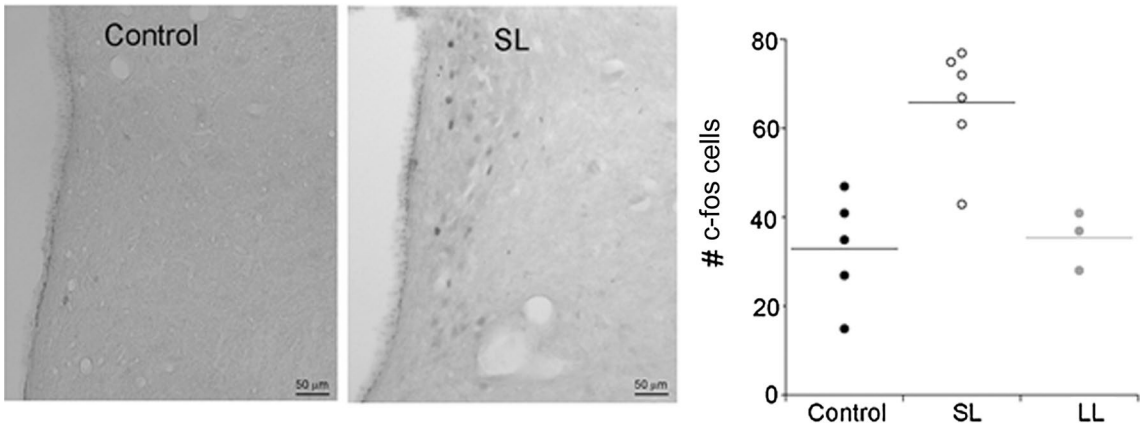

Fig. 6 Activation of locus coeruleus (LC) neurons following repeated exposure to resident–intruder stress. Representative bright-field photomicrographs from a control rat exposed (control) to 5-day repeated manipulations (SL). Scatterplot showing the number of c-fos profiles in the LC after the fifth stress or control manipulation for individual control, SL and LL rats. Lines through the points indicate the group mean (control $n=5$; SL $n=6$; LL $n=3$)

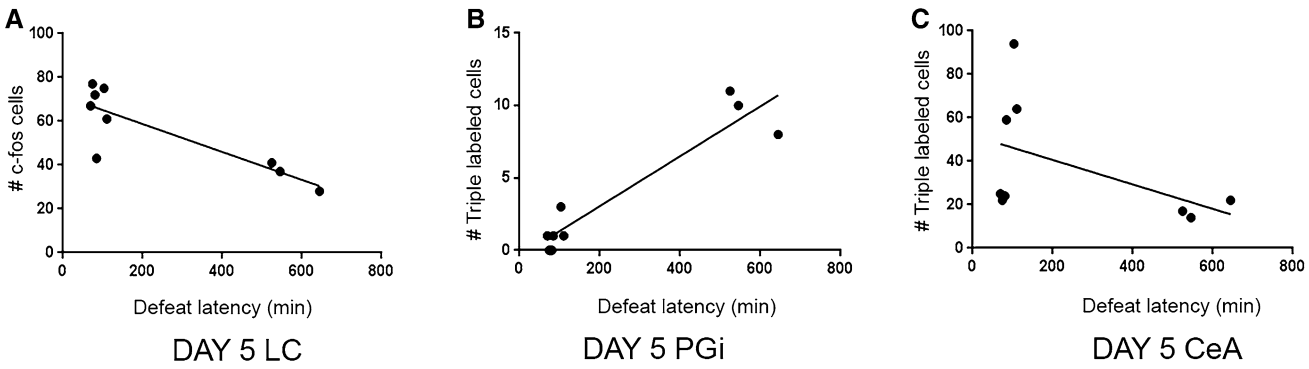

Fig. 7 Correlation studies on the number of c-fos in LC (**a**), triple-labeled neurons in the PGi (**b**) and triple-labeled neurons in the CeA (**c**) with respect to the latency to defeat. The number of c-fos in LC showed a significant positive correlation with the defeat latency. A positive correlation was also observed on the number of triple-labeled neurons in the PGi

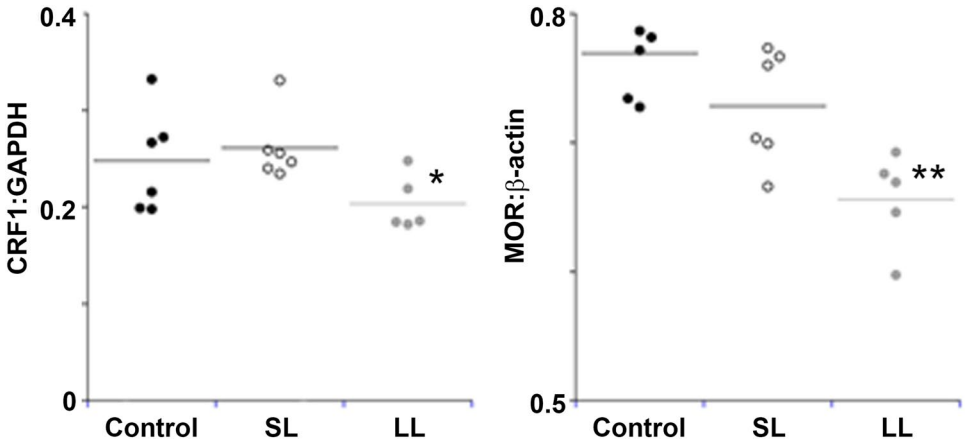

Fig. 8 Western blot analysis of CRF receptor 1 (CRF1) and mu-opioid receptor (MOR) in the locus coeruleus in control rats or rats that were exposed to repeated social stress and were classified as short (SL) or long latency (LL). Scatter plot showing the mean ratio of the integrated intensity of each band of CRF1 or MOR protein to the corresponding GAPDH band from the same sample. *$p<0.05$ vs SL; **$p<0.001$ vs SL and control. (control $n=5$; SL $n=6$; LL $n=5$)

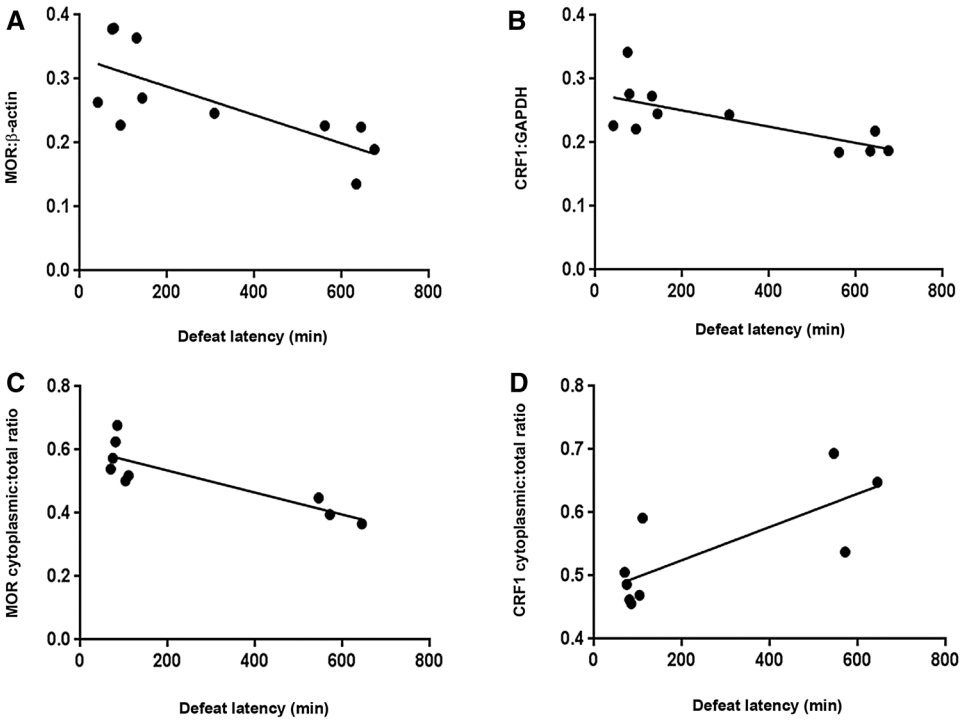

Fig. 9 Correlation studies on the MOR and CRF1 protein expression levels in LC (**a, b**) and MOR and CRF1 cytoplasmic:total ratio in LC (**c, d**) with respect to the latency to defeat. A positive correlation was observed between the MOR protein expression level and latency to defeat. Similar, positive correlation was observed between CRF1 protein expression level and latency to defeat. While the MOR cytoplasmic:total ratio was negatively correlated with defeat latency, the CRF1 cytoplasmic:total ratio was positive correlated with defeat latency

et al. 2008). Thus, all female rats used in these studies were not examined for the phase of estrous cycle.

Using the preembedding immunogold method for electron microscopy provides distinct subcellular localization of reaction product and allows optimal preservation of ultrastructural morphology. However, some caveats are inherent to this technique, including antibody penetration because of the relative thickness of the tissue (Leranth and Pickel 1989) and this may result in underestimation of the relative frequencies of the marker's distribution. To minimize this caveat, ultrathin tissue sections were collected near the tissue–Epon interface, where penetration was optimal, so that the CRF1 or MOR immunoreactivity was clearly detectable in all sections used for analysis. In addition, sampling of profiles was conducted only when CRF1 or MOR is present. In addition, all experimental groups were processed in parallel, so that this caveat should not contribute to group differences.

Acute social stress effects on the LC and its afferent circuitry

Previous electrophysiological studies demonstrated that during acute stress, LC neurons are co-regulated by CRF-mediated excitation and opioid-mediated inhibition in an opposing manner and that CRF excitation predominates (Curtis et al. 2001, 2012). Specifically, LC neurons become activated during stress and pretreatment with a CRF antagonist prevents this activation and unmasks an opioid-mediated inhibition (Curtis et al. 2001, 2012). The opioid influence may serve to restrain activation or to promote recovery after the stressor is terminated. For example, administration of the opioid antagonist, naloxone, prior to hypotensive stress results in a slower return of LC activity to baseline after stressor termination (Curtis et al. 2001). CRF and enkephalin axon terminals converge onto LC dendrites and LC dendrites exhibit immunolabeling for CRF_1 and MOR (Van Bockstaele et al. 1996a, b; Xu et al. 2004; Reyes et al. 2006). The CeA and PGi are primary sources of CRF and ENK projections to the LC, respectively (Drolet et al. 1992; Van Bockstaele et al. 1998; Tjoumakaris et al. 2003).

In the present study, using c-fos as a marker of neuronal activity, acute resident–intruder stress engaged both excitatory CRF afferents to the LC and inhibitory ENK afferents to the LC. This is consistent with previous electrophysiological studies of acute exposure to hypotensive stress and predator odor (Curtis et al. 2001, 2012), underscoring that this is a shared circuitry for LC regulation by acute stressors. Importantly, the present study provided evidence for anatomical localization of sources of CRF and ENK afferents involved in this regulation. The present results using female rats were identical to those found in males, indicating that this effect is highly reproducible and there is no apparent sex difference (Reyes et al. 2015).

Repeated social stress effects on the LC and its afferent circuitry

With repeated social stress, two phenotypes emerge characterized by their propensity to assume the subordinate defeat posture (Wood et al. 2010, 2015; Chen et al. 2015;

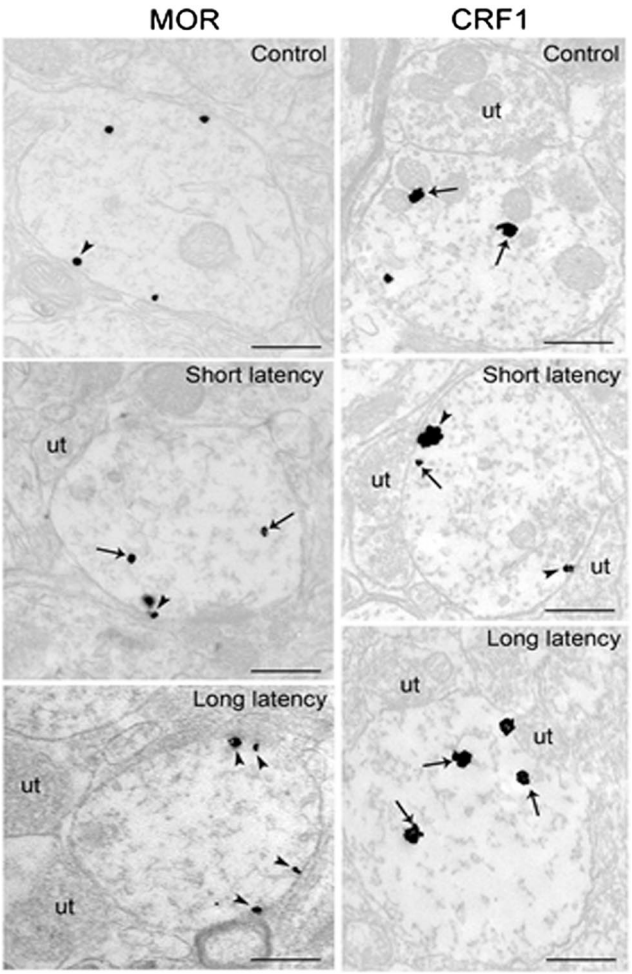

Fig. 10 Electron microscopic evidence for repeated social stress-induced re-distribution of mu-opioid receptor (MOR) and CRF receptor 1 (CRF1) in the rat LC. Left panels show a dendrite from a control rat that contains immunogold–silver labeling for MOR along the plasmalemma is depicted by arrowhead. MOR within the cytoplasmic compartment is depicted by arrows. Left panel (middle) shows MOR labeling in a dendrite from a SL rat. Immunogold–silver labeling for MOR (arrows) can be predominantly seen within the cytoplasmic compartment, although some MOR immunogold–silver particles are localized along the plasma membrane (arrowhead). Left panels illustrate that immunogold–silver labeling for MOR shifts from plasmalemma to the cytoplasmic compartment in SL rat. Right panels show immunogold–silver labeling for CRF1. Right panel (middle) shows that CRF1 labeling shifts from cytoplasmic compartment to plasmalemmal localization in SL rat. Right panel (bottom) shows CRF1 within the cytoplasmic compartment in LL rats. Scale bars, 0.5 µm

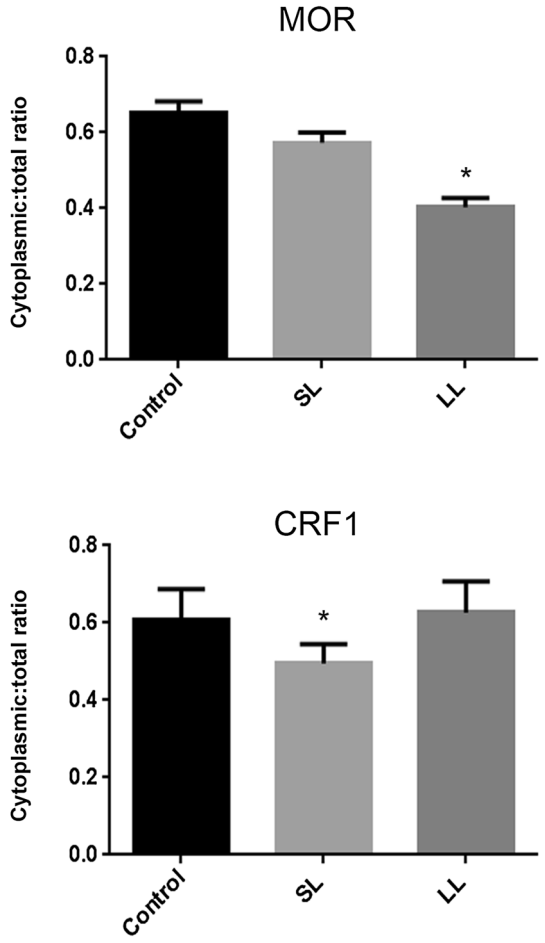

Fig. 11 Quantification of the ratio of cytoplasmic to total MOR and CRF1 labeling in the LC dendrites of female rats following social defeat exposure. Bars represent the mean ratio of cytoplasmic to total ratio of MOR and CRFr in control, SL and LL rats. Values are means ± SEM of 3–6 rats per group (control $n=6$; SL $n=6$ and LL $n=3$). *$p<0.001$ compared with other groups

Pearson-Leary et al. 2017). In addition to their different responses to the stress, these phenotypes are characterized by different stress consequences. For example, the SL phenotype was characterized by increased depressive-like behaviors and anxiety-like behaviors and increased neuroendocrine endpoints of stress vulnerability compared to the LL phenotype (Wood et al. 2010, 2015; Chen et al. 2015; Pearson-Leary et al. 2017). In the present study, resident–intruder stress shifted the balance of LC regulation towards CRF excitation in SL rats and opioid inhibition in LL rats and this was expressed as the maintenance of stress-induced activation in SL rats and its loss in LL rats. These findings are largely similar to those in male rats (Reyes et al. 2015) and further support the interpretation that establishment of different coping strategies is associated with strategy-specific changes in the neural circuitry that regulates the LC-NE stress response system.

Repeated social stress, CRF1, and MOR

Although repeated social stress produced similar shifts in the CRF/ENK regulation of LC activity in female rats as reported for males, sex differences were apparent in the effects of stress on receptor expression and trafficking. In male LL rats, repeated social stress decreased

CRF1 and increased MOR expression, effects that would further favor ENK inhibition in this phenotype (Reyes et al. 2015). In female LL rats, repeated social stress also decreased CRF1 expression; however, it decreased MOR expression as well. This could lessen the impact of an enhanced ENK input. Although these findings are suggestive of sex differences, an analysis of males and females in the same study is necessary to conclude this.

Evidence for CRF release in the LC would be predicted to be associated with increased CRF1 internalization. In male rats, local CRF infusion into the LC and swim stress increases the ratio of cytoplasmic:total CRF1-immunolabeling in LC dendrites, indicative of internalization (Reyes et al. 2006, 2008, 2015; Bangasser et al. 2010). Consistent with CRF release in the LC of male SL rats exposed to repeated resident–intruder stress, the ratio of cytoplasmic:total CRF1-immunolabeling was also increased in LC dendrites (Reyes et al. 2015). Notably, there is similar evidence for CRF1 internalization in LC dendrites of male CRF-overexpressing mice (Bangasser and Valentino 2012). In contrast, evidence argues against stress- and agonist-induced CRF1 internalization in females and rather suggests that these conditions result in recruitment of CRF1 to the plasma membrane as indicated by a decreased ratio of cytoplasmic:total CRF1-immunolabeling (Bangasser et al. 2010; Bangasser and Valentino 2012). The present finding that the cytoplasmic:total CRF1 ratio decreases in SL females as it does in female rats exposed to swim stress or CRF-overexpressing mice is consistent with increased CRF release in this phenotype. Immunoprecipitation studies showing a decreased association of CRF1 with β-arrestin2 in females compared to males implicated this as a possible molecular mechanism for sex differences in CRF1 trafficking (Bangasser et al. 2010).

Evidence for increased ENK release in female LL rats would predict MOR internalization as was reported for male LL rats. However, as was the case for CRF1 in female SL rats, there was evidence of MOR recruitment to the plasma membrane. Increased MOR on the plasma membrane may counter the decreased MOR protein expression in this phenotype, so that increased ENK release in the LC may be effective in restraining LC activation during stress. Notably, evidence for CRF1 and MOR trafficking in opposing directions dependent on sex has important implications, particularly given recent evidence for MOR signaling in intracellular compartments (Stoeber et al. 2018). Future investigations that directly compare agonist- and stress-induced MOR trafficking in males and females may reveal this as a cellular basis for sex differences in sensitivity to stress and opioids.

Functional implications

Activation of the forebrain norepinephrine system is part of the cognitive limb of the stress response. Maintaining the appropriate balance of CRF/ENK regulation keeps the magnitude and duration of this response optimal. Whereas a diminished response could increase risk of immediate harm, an excessive and prolonged response sets the stage for allostasis and stress-related pathology. Together with the previous findings using male rats, the present results confirm that repeated social stress shifts the CRF/ENK balance of LC regulation in opposing directions in rats with different coping strategies related to their propensity to become subordinate. The loss of LC activation in rats that resist subordination may confer a resilience to repeated stress as a result of an enhanced ENK inhibitory drive. In contrast, the loss of this inhibitory influence in more subordinate rats may decrease resilience and increase vulnerability to stress-related disorders that are characterized by arousal symptoms, such as post-traumatic stress disorder. In addition, these individuals may be more prone to opioid abuse as a lower endogenous opioid influence could fuel a drive for self-medication. Intriguing potential sex differences in stress-induced regulation of receptor expression and trafficking should be a basis for examining sex differences in these endpoints in a systematic manner.

Compliance with ethical standards

Conflict of interest We have nothing to disclose in terms of disclosure of potential conflicts of interest.

Research involving human and/or animal participants All studies were approved by the Children's Hospital of Philadelphia Institutional Animal Care and Use Committee and conformed to the guidelines set forth by the National Institutes of Health Guide for the Use of Laboratory Animals.

Informed consent Informed consent was obtained from all authors included in the study.

References

Andrezik JA, Chan-Palay V, Palay SL (1981) The nucleus paragigantocellularis lateralis in the rat. Conformation and cytology. Anat Embryol (Berl) 161:355–371

Avgustinovich DF, Kovalenko IL, Kudryavtseva NN (2005) A model of anxious depression: persistence of behavioral pathology. Neurosci Behav Physiol 35:917–924

Bangasser DA, Valentino RJ (2012) Sex differences in molecular and cellular substrates of stress. Cell Mol Neurobiol 32:709–723

Bangasser DA, Curtis A, Reyes BA, Bethea TT, Parastatidis I, Ischiropoulos H, Van Bockstaele EJ, Valentino RJ (2010) Sex differences in corticotropin-releasing factor receptor signaling

and trafficking: potential role in female vulnerability to stress-related psychopathology. Mol Psychiatry 15(877):896–904
Barr J, Van Bockstaele EJ (2005) Vesicular glutamate transporter-1 colocalizes with endogenous opioid peptides in axon terminals of the rat locus coeruleus. Anat Rec 284:466–474
Berridge CW, Waterhouse BD (2003) The locus-coeruleus-noradrenergic system: modulation of behavioral state and state-dependent cognitive processes. Brain Res Rev 42:33–84
Bissette G, Klimek V, Pan J, Stockmeier C, Ordway G (2003) Elevated concentrations of CRF in the locus coeruleus of depressed subjects. Neuropsychopharmacology 28:1328–1335
Breen KM, Davis TL, Doro LC, Nett TM, Oakley AE, Padmanabhan V, Rispoli LA, Wagenmaker ER, Karsch FJ (2008) Insight into the neuroendocrine site and cellular mechanism by which cortisol suppresses pituitary responsiveness to gonadotropin-releasing hormone. Endocrinology 149:767–773
Chaijale NN, Curtis AL, Wood SK, Zhang XY, Bhatnagar S, Reyes BA, Van Bockstaele EJ, Valentino RJ (2013) Social stress engages opioid regulation of locus coeruleus norepinephrine neurons and induces a state of cellular and physical opiate dependence. Neuropsychopharmacology 38:1833–1843
Chen RJ, Kelly G, Sengupta A, Heydendael W, Nicholas B, Beltrami S, Luz S, Peixoto L, Abel T, Bhatnagar S (2015) MicroRNAs as biomarkers of resilience or vulnerability to stress. Neuroscience 305:36–48
Cheng PY, Moriwaki A, Wang JB, Uhl GR, Pickel VM (1996) Ultrastructural localization of mu-opioid receptors in the superficial layers of the rat cervical spinal cord: extrasynaptic localization and proximity to Leu5-enkephalin. Brain Res 731:141–154
Curtis AL, Lechner SM, Pavcovich LA, Valentino RJ (1997) Activation of the locus coeruleus noradrenergic system by intracoerulear microinfusion of corticotropin-releasing factor: effects on discharge rate, cortical norepinephrine levels and cortical electroencephalographic activity. J Pharmacol Exp Ther 281:163–172
Curtis AL, Bello NT, Valentino RJ (2001) Evidence for functional release of endogenous opioids in the locus ceruleus during stress termination. J Neurosci 21:RC152
Curtis AL, Leiser SC, Snyder K, Valentino RJ (2012) Predator stress engages corticotropin-releasing factor and opioid systems to alter the operating mode of locus coeruleus norepinephrine neurons. Neuropharmacology 62:1737–1745
Dai X, Noga BR, Douglas JR, Jordan LM (2005) Localization of spinal neurons activated during locomotion using the c-fos immunohistochemical method. J Neurophysiol 93:3442–3452
de Kloet ER, Joels M, Holsboer F (2005) Stress and the brain: from adaptation to disease. Nat Rev Neurosci 6:463–475
Drolet G, Van Bockstaele EJ, Aston-Jones G (1992) Robust enkephalin innervation of the locus coeruleus from the rostral medulla. J Neurosci 12:3162–3174
Ehnert K, Moberg GP (1991) Disruption of estrous behavior in ewes by dexamethasone or management-related stress. J Animal Science 69:2988–2994
Enman NM, Reyes BAS, Shi Y, Valentino RJ, Van Bockstaele EJ (2018) Sex differences in morphine-induced trafficking of mu-opioid and corticotropin-releasing factor receptors in locus coeruleus neurons. Brain Res. https://doi.org/10.1016/j.brainres.2018.11.001
Flannelly KJ, Flannelly L (1987) Time course of postpartum aggression in rats (*Rattus norvegicus*). J Comp Psychol 101:101–103
Ghosal K, Naples SP, Rabe AR, Killian KA (2010) Agonistic behavior and electrical stimulation of the antennae induces Fos-like protein expression in the male cricket brain. Arch Insect Biochem Physiol 74:38–51
Gold PW, Chrousos GP (2002) Organization of the stress system and its dysregulation in melancholic and atypical depression: high vs low CRH/NE states. Mol Psychiatry 7:254–275
Gonzalez AS, Rodriguez Echandia EL, Cabrera R, Foscolo MR (1994) Neonatal chronic stress induces subsensitivity to chronic stress in adult rats: II. Effects on estrous cycle in females. Physiol Behav 56:591–595
Gorenstein C, Bundman MC, Lew PJ, Olds JL, Ribak CE (1985) Dendritic transport. I. Colchicine stimulates the transport of lysosomal enzymes from cell bodies to dendrites. J Neurosci 5:2009–2017
Grillon C, Southwick SM, Charney DS (1996) The psychobiological basis of posttraumatic stress disorder. Mol Psychiatry 1:278–297
Guajardo HM, Snyder K, Ho A, Valentino RJ (2017) Sex differences in mu-opioid receptor regulation of the rat locus coeruleus and their cognitive consequences. Neuropsychopharmacology 42:1295–1304
Jia Y, Yao H, Zhou J, Chen L, Zeng Q, Yuan H, Shi L, Nan X, Wang Y, Yue W, Pei X (2011) Role of epimorphin in bile duct formation of rat liver epithelial stem-like cells: involvement of small G protein RhoA and C/EBPbeta. J Cellular Physiol 226:2807–2816
Koolhaas JM, Korte SM, De Boer SF, Van Der Vegt BJ, Van Reenen CG, Hopster H, De Jong IC, Ruis MA, Blokhuis HJ (1999) Coping styles in animals: current status in behavior and stress-physiology. Neurosci Biobehav Rev 23:925–935
Kravets JL, Reyes BA, Unterwald EM, Van Bockstaele EJ (2015) Direct targeting of peptidergic amygdalar neurons by noradrenergic afferents: linking stress-integrative circuitry. Brain Struct Funct 220:541–558
Leranth C, Pickel VM (1989) Electron microscopic preembedding double-labeling methods. In: Heimer L, Zaborszky L (eds) Neuroanatomical tracing methods, vol 2, 1st edn. Plenum Press, New York, pp 129–172
Li XF, Hu MH, Li SY et al (2014) Overexpression of corticotropin releasing factor in the central nucleus of the amygdala advances puberty and disrupts reproductive cycles in female rats. Endocrinology 155:3934–3944
Marchlewska-Koj A, Pochron E, Galewicz-Sojecka A, Galas J (1994) Suppression of estrus in female mice by the presence of conspecifics or by foot shock. Physiol Behav 55:317–321
Matsuzaki H, Izumi T, Horinouchi T, Boku S, Inoue T, Yamaguchi T, Yoshida T, Matsumoto M, Togashi H, Miwa S, Koyama T, Yoshioka M (2011) Juvenile stress attenuates the dorsal hippocampal postsynaptic 5-HT1A receptor function in adult rats. Psychopharmacology (Berl) 214:329–337
McEwen BS (1998) Stress, adaptation, and disease. Allostasis and allostatic load. Ann N Y Acad Sci 840:33–44
Melia KR, Duman RS (1991) Involvement of corticotropin-releasing factor in chronic stress regulation of the brain noradrenergic system. Proc Natl Acad Sci USA 88:8382–8386
Miczek KA (1979) A new test for aggression in rats without aversive stimulation: differential effects of *d*-amphetamine and cocaine. Psychopharmacology 60:253–259
Miczek KA, Covington HE III, Nikulina EM Jr, Hammer RP (2004) Aggression and defeat: persistent effects on cocaine self-administration and gene expression in peptidergic and aminergic mesocorticolimbic circuits. Neurosci Biobehav Rev 27:787–802
Miczek KA, Thompson ML, Shuster L (1982) Opioid-like analgesia in defeated mice. Science 215:1520–1522
Milner TA, Okada J, Pickel VM (1995) Monosynaptic input from Leu5-enkephalin-immunoreactive terminals to vagal motor neurons in the nucleus ambiguus: comparison with the dorsal motor nucleus of the vagus. J Comp Neurol 353:391–406
Monti-Graziadei AG, Berkley KJ (1991) Effects of colchicine on retrogradely-transported WGA-HRP. Brain Res 565:162–166
Nikulina EM, Hammer RP Jr, Miczek KA, Kream RM (1999) Social defeat stress increases expression of mu-opioid receptor mRNA in rat ventral tegmental area. Neuroreport 10:3015–3019
Nikulina EM, Arrillaga-Romany I, Miczek KA, Hammer RP Jr (2008) Long-lasting alteration in mesocorticolimbic structures after

repeated social defeat stress in rats: time course of mu-opioid receptor mRNA and FosB/DeltaFosB immunoreactivity. Eur J Neurosci 27:2272–2284

Noga BR, Johnson DM, Riesgo MI, Pinzon A (2011) Locomotor-activated neurons of the cat. II. Noradrenergic innervation and colocalization with NEalpha 1a or NEalpha 2b receptors in the thoraco-lumbar spinal cord. J Neurophysiol 105:1835–1849

Paxinos G, Watson C (1998) The rat brain in stereotaxic coordinates, 2nd edn. Academic Press, North Ryde

Pearson-Leary J, Eacret D, Chen R, Takano H, Nicholas B, Bhatnagar S (2017) Inflammation and vascular remodeling in the ventral hippocampus contributes to vulnerability to stress. Transl Psychiatry 7:e1160

Peng J, Sarkar S, Chang SL (2012) Opioid receptor expression in human brain and peripheral tissues using absolute quantitative real-time RT-PCR. Drug Alcohol Depend 124:223–228

Pierce BN, Hemsworth PH, Rivalland ET, Wagenmaker ER, Morrissey AD, Papargiris MM, Clarke IJ, Karsch FJ, Turner AI, Tilbrook AJ (2008) Psychosocial stress suppresses attractivity, proceptivity and pulsatile LH secretion in the ewe. Horm Behav 54:424–434

Pietrzak RH, Gallezot JD, Ding YS, Henry S, Potenza MN, Southwick SM, Krystal JH, Carson RE, Neumeister A (2013) Association of posttraumatic stress disorder with reduced in vivo norepinephrine transporter availability in the locus coeruleus. JAMA Psychiatry 70:1199–1205

Por E, Byun HJ, Lee EJ, Lim JH, Jung SY, Park I, Kim YM, Jeoung DI, Lee H (2010) The cancer/testis antigen CAGE with oncogenic potential stimulates cell proliferation by up-regulating cyclins D1 and E in an AP-1- and E2F-dependent manner. J Biol Chem 285:14475–14485

Retson TA, Hoek JB, Sterling RC, Van Bockstaele EJ (2015) Amygdalar neuronal plasticity and the interactions of alcohol, sex, and stress. Brain Struct Funct 220:3211–3232

Reyes BA, Valentino RJ, Xu G, Van Bockstaele EJ (2005) Hypothalamic projections to locus coeruleus neurons in rat brain. Eur J Neurosci 22:93–106

Reyes BAS, Fox K, Valentino RJ, Van Bockstaele EJ (2006) Agonist-induced internalization of corticotropin-releasing factor receptors in noradrenergic neurons of the rat locus coeruleus. Eur J Neurosci 23:2991–2998

Reyes BA, Valentino RJ, Van Bockstaele EJ (2008) Stress-induced intracellular trafficking of corticotropin-releasing factor receptors in rat locus coeruleus neurons. Endocrinology 149:122–130

Reyes BA, Carvalho AF, Vakharia K, Van Bockstaele EJ (2011) Amygdalar peptidergic circuits regulating noradrenergic locus coeruleus neurons: linking limbic and arousal centers. Exp Neurol 230:96–105

Reyes BA, Zitnik G, Foster C, Van Bockstaele EJ, Valentino RJ (2015) Social stress engages neurochemically-distinct afferents to the rat locus coeruleus depending on coping strategy. eNeuro. https://doi.org/10.1523/ENEURO.0042-15.2015. **(eCollection 2015)**

Rite I, Venero JL, Tomas-Camardiel M, Machado A, Cano J (2003) Expression of BDNF mRNA in substantia nigra is dependent on target integrity and independent of neuronal activation. J Neurochem 87:709–721

Rygula R, Abumaria N, Flugge G, Fuchs E, Ruther E, Havemann-Reinecke U (2005) Anhedonia and motivational deficits in rats: impact of chronic social stress. Behav Brain Res 162:127–134

Stoeber M, Jullie D, Lobingier BT, Laeremans T, Steyaert J, Schiller PW, Manglik A, von Zastrow M (2018) A genetically encoded biosensor reveals location bias of opioid drug action. Neuron 98:963–976 e965

Surratt CK, Johnson PS, Moriwaki A, Seidleck BK, Blaschak CJ, Wang JB, Uhl GR (1994) -mu opiate receptor. Charged transmembrane domain amino acids are critical for agonist recognition and intrinsic activity. J Biol Chem 269:20548–20553

Sutherland JE, Burian LC, Covault J, Conti LH (2010) The effect of restraint stress on prepulse inhibition and on corticotropin-releasing factor (CRF) and CRF receptor gene expression in Wistar–Kyoto and Brown Norway rats. Pharmacol Biochem Behav 97:227–238

Teskey GC, Kavaliers M, Hirst M (1984) Social conflict activates opioid analgesic and ingestive behaviors in male mice. Life Sci 35:303–315

Tjoumakaris SI, Rudoy C, Peoples J, Valentino RJ, Van Bockstaele EJ (2003) Cellular interactions between axon terminals containing endogenous opioid peptides or corticotropin-releasing factor in the rat locus coeruleus and surrounding dorsal pontine tegmentum. J Comp Neurol 466:445–456

Valentino RJ, Van Bockstaele E (2008) Convergent regulation of locus coeruleus activity as an adaptive response to stress. Eur J Pharmacol 583:194–203

Van Bockstaele EJ, Branchereau P, Pickel VM (1995) Morphologically heterogeneous met-enkephalin terminals form synapses with tyrosine hydroxylase-containing dendrites in the rat nucleus locus coeruleus. J Comp Neurol 363:423–438

Van Bockstaele EJ, Colago EEO, Cheng P, Moriwaki A, Uhl GR, Pickel VM (1996a) Ultrastructural evidence for prominent distribution of the mu-opioid receptor at extrasynaptic sites on noradrenergic dendrites in the rat nucleus locus coeruleus. J Neurosci 16:5037–5048

Van Bockstaele EJ, Colago EEO, Moriwaki A, Uhl GR (1996b) Mu-opioid receptor is located on the plasma membrane of dendrites that receive asymmetric synapses from axon terminals containing leucine-enkephalin in the rat nucleus locus coeruleus. J Comp Neurol 376:65–74

Van Bockstaele EJ, Colago EEO, Valentino RJ (1996c) Corticotropin-releasing factor-containing axon terminals synapse onto catecholamine dendrites and may presynaptically modulate other afferents int he rostral pole of the nucleus locus coeruleus in the rat brain. J Comp Neurol 364:523–534

Van Bockstaele EJ, Colago EE, Valentino RJ (1998) Amygdaloid corticotropin-releasing factor targets locus coeruleus dendrites: substrate for the co-ordination of emotional and cognitive limbs of the stress response. J Neuroendocrinol 10:743–757

Ventura C, Bastagli L, Bernardi P, Caldarera CM, Guarnieri C (1989) Opioid receptors in rat cardiac sarcolemma: effect of phenylephrine and isoproterenol. Biochem Biophys Acta 987:69–74

Ver Hoeve ES, Kelly G, Luz S, Ghanshani S, Bhatnagar S (2013) Short-term and long-term effects of repeated social defeat during adolescence or adulthood in female rats. Neuroscience 249:63–73

Vicario M, Alonso C, Guilarte M, Serra J, Martinez C, Gonzalez-Castro AM, Lobo B, Antolin M, Andreu AL, Garcia-Arumi E, Casellas M, Saperas E, Malagelada JR, Azpiroz F, Santos J (2012) Chronic psychosocial stress induces reversible mitochondrial damage and corticotropin-releasing factor receptor type-1 upregulation in the rat intestine and IBS-like gut dysfunction. Psychoneuroendocrinology 37:65–77

Wong ML, Kling MA, Munson PJ, Listwak S, Licinio J, Prolo P, Karp B, McCutcheon IE, Geracioti TD Jr, DeBellis MD, Rice KC, Goldstein DS, Veldhuis JD, Chrousos GP, Oldfield EH, McCann SM, Gold PW (2000) Pronounced and sustained central hypernoradrenergic function in major depression with melancholic features: relation to hypercortisolism and corticotropin-releasing hormone. Proc Natl Acad Sci USA 97:325–330

Wood SK, Baez MA, Bhatnagar S, Valentino RJ (2009) Social stress-induced bladder dysfunction: potential role of corticotropin-releasing factor. Am J Physiol Regul Integr Comp Physiol 296:R1671–R1678

Wood SK, Walker HE, Valentino RJ, Bhatnagar S (2010) Individual differences in reactivity to social stress predict susceptibility and

resilience to a depressive phenotype: role of corticotropin-releasing factor. Endocrinology 151:1795–1805

Wood SK, McFadden KV, Grigoriadis D, Bhatnagar S, Valentino RJ (2012) Depressive and cardiovascular disease comorbidity in a rat model of social stress: a putative role for corticotropin-releasing factor. Psychopharmacology 222:325–336

Wood SK, Wood CS, Lombard CM, Lee CS, Zhang XY, Finnell JE, Valentino RJ (2015) Inflammatory factors mediate vulnerability to a social stress-induced depressive-like phenotype in passive coping rats. Biol Psychiatry 78:38–48

Xu G-P, Van Bockstaele EJ, Reyes BA, Bethea T, Valentino RJ (2004) Chronic morphine sensitizes the brain norepinephrine system to corticotropin-releasing factor and stress. J Neurosci 24:8193–8197